

Radiation-Induced Polymerizations in Continuous Stirred-Tank Reactors

H. T. CHEN

Newark College of Engineering, Newark, New Jersey

and

F. B. HILL

Brookhaven National Laboratory, Upton, New York

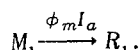
A theoretical study of the performance characteristics of continuous stirred-tank reactors when used to conduct radiation-induced polymerizations is presented. The effects on conversion and molecular weight distribution of the interaction of radiation attenuation, chemical kinetics, and mixing are examined for initiation by ultraviolet light and by Co^{60} gamma radiation.

Initiation of chemical reactions by radiation has as one of its distinguishing features spatial nonuniformities resulting from radiation attenuation. Many factors influence the degree to which these nonuniformities affect reactor performance. These factors include reaction mechanism, reactor type and size, the type of radiation, the presence or absence of a photocatalyst, and mixing state. The influence of these factors on reaction rates or conversion has been examined in previous papers (1 to 5). In the present paper the analysis is extended to include effects on molecular weight distribution in addition polymerization as well as effects on reaction rate or conversion.

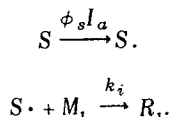
REACTION MECHANISM

The reaction mechanism to be considered is that of addition polymerization in bulk. We will treat the following three different initiation modes, one of which will be operative at a time:

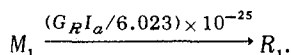
Initiation by direct absorption of ultraviolet light by monomer



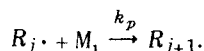
Initiation by absorption of ultraviolet light by sensitizer



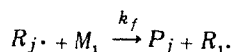
Initiation by absorption of ionizing radiation by monomer



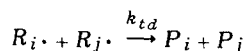
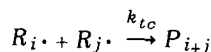
The remaining steps in the mechanism are
Propagation



Chain transfer to monomer



Termination by combination and disproportionation



It is assumed that the rate constants k_p , k_f , k_{td} , and k_{tc} are constant and independent of chain length. Depolymerization and chain branching are assumed to be absent.

ABSORBED INTENSITY DISTRIBUTION

The reaction takes place in a continuous stirred-tank reactor of annular geometry with a line source of monochromatic radiation located on its axis (see Figure 1). For present purposes the line source will be assumed to be effectively infinite in length. This assumption is a good one for thin reactors. For thick reactors the degree of nonuniformity in the initiation rate distribution will be underestimated. A correct qualitative evaluation of the effects of nonuniformities will nevertheless be found.

For the geometry shown in Figure 1, the contribution dl to the total intensity at radial position z from the source segment dl is (6)

$$dl = \frac{S_L e^{-\mu(z-z_1) \sec \theta}}{4\pi z} d\theta \quad (1)$$

It is implicit in Equation (1) that there are no effects of reflection or refraction, and, in the case of ionizing radiation, there are no buildup effects due to scattered radiation.

The total intensity at radial position z is obtained by integrating Equation (1) over all values of θ .

$$I = (2S_L / 4\pi z) \int_0^{\pi/2} e^{-\mu(z-z_1) \sec \theta} d\theta \quad (2)$$

Since at $z = z_1$, $I = I_0$, then

$$S_L = 4I_0 z_1$$

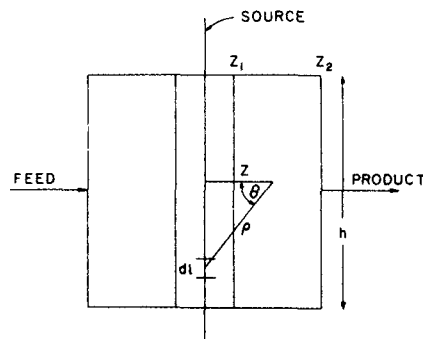


Fig. 1. Schematic diagram of reactor.

and Equation (2) becomes

$$I = (2/\pi)(z_1 I_0/z) \int_0^{\pi/2} e^{-\mu(z-z_1)\sec \theta} d\theta \quad (3)$$

The volumetric rate of absorption of radiation energy is μI , or

$$I_a = \mu(2/\pi)(z_1 I_0/z) \int_0^{\pi/2} e^{-\mu(z-z_1)\sec \theta} d\theta \quad (3a)$$

A different interpretation is given to μ , depending on the mode of initiation. For direct photoinitiation resulting from absorption of ultraviolet light by monomer $\mu = \alpha_m m$. When a sensitizer is present, which upon absorption of ultraviolet light dissociates to produce free radicals, which in turn serve to initiate the polymerization, then $\mu = \alpha_s s$. In initiation by Co^{60} gamma rays, a process which is relatively insensitive to detailed chemical composition, μ is taken to be simply the linear absorption coefficient. Thus in both modes of initiation via absorption of ultraviolet light, the intensity changes with conversion (of monomer or sensitizer), whereas in the case of ionizing radiation the intensity does not vary with extent of conversion. For initiation via ultraviolet light then the equation for the absorbed intensity, Equation (3a), is coupled to a mass balance for sensitizer or for monomer.

REACTOR EQUATIONS

For the reactor shown in Figure 1, we will assume that the feed consists of monomer and dissolved sensitizer. Equations will be presented for this situation although they will be valid also when sensitizer is absent by setting the sensitizer concentration equal to zero. The lifetime of the monomer and sensitizer will be taken to be long compared with the mixing time in the reactor so that the concentration of these substances will be uniform throughout the reactor. It will be assumed that the steady state approximation with respect to reactive intermediates applies throughout the reactor. Finally, two extreme mixing states with respect to chain centers will be considered. In one, which will be referred to as the perfect mixing (PM) state, the centers are uniformly mixed throughout the reactor. The mean chain lifetime is long compared with the mixing time in the reactor, and the effective initiation rate is the average rate. For the opposite extreme mixing state, the no mixing (NM) state, the centers are born and die at the same location, subject to the local initiation rate. The mean chain lifetime is short compared with the mixing time. Hill and Felder (1) have shown that under these circumstances, at small conversions, the transition from the NM state to the PM state leads to increased conversion. Jacob and Dranoff (7) find this fact to be true at finite conversions also.

Perfect Mixing (PM)

For the case of sensitized initiation, material balances for sensitizer, monomer, chain centers, and dead polymer are

$$qs_0 - qs - \bar{\Omega}V = 0 \quad (4)$$

$$qm_0 - qm + V(-k_p m \bar{\Sigma} r_i - k_f m \bar{\Sigma} r_i) = 0 \quad (5)$$

$$\bar{\Omega} - (k_{tc} + k_{td}) (\bar{\Sigma} r_i)^2 = 0 \quad (6)$$

$$\bar{\Omega} - k_p r_1 m - (k_{tc} + k_{td}) r_1 \bar{\Sigma} r_i - k_f m r_1 + k_f m \bar{\Sigma} r_i = 0 \quad (7)$$

$$k_p m (r_{j-1} - r_j) - (k_{tc} + k_{td}) r_j \bar{\Sigma} r_i - k_f m r_j = 0 \quad (8)$$

where $j = 2, 3, \dots \infty$

$$-qp_j + (k_{td} r_j \bar{\Sigma} r_i + \frac{1}{2} k_{tc} \sum_{i=1}^{j-1} r_i r_{j-i} + k_f m r_j) V = 0 \quad (9)$$

where $j = 1, 2, 3, \dots \infty$

where $\bar{\Sigma} r_i$ = total polymer radical concentration, and $\bar{\Omega}$ represents the effective initiation rate given by

$$\bar{\Omega} = \frac{2}{(z_2^2 - z_1^2)} \int_{z_1}^{z_2} z \Omega(z) dz \quad (10)$$

and

$$\Omega(z) = \phi_s I_a(z)$$

Equation (4) may be written as

$$s = s_0 - \theta \bar{\Omega} \quad (11)$$

where $\theta = V/q$. If we combine Equations (5) and (6) we obtain

$$m = \frac{m_0}{1 + \theta(k_p + k_f)(\bar{\Omega}/k_t)^{1/2}} \quad (12)$$

From Equations (6), (7), and (8) one finds

$$r_j = \left[\frac{k_p m}{m(k_p + k_f) + (k_t \bar{\Omega})^{1/2}} \right]^{j-1} r_1 \quad (13)$$

where

$$r_1 = \frac{\bar{\Omega} + k_f m (\bar{\Omega}/k_t)^{1/2}}{m(k_p + k_f) + (k_t \bar{\Omega})^{1/2}} \quad (14)$$

From Equation (9) the effluent concentration p_j is

$$p_j = \theta r_j [k_{td} (\bar{\Omega}/k_t)^{1/2} + k_f m] + \frac{\theta}{2} k_{tc} \sum_{i=1}^{j-1} r_i r_{j-i} \quad (15)$$

By the aid of Euler summation formulas (8), Equation (15) becomes

$$p_j = \theta r_j [k_{td} (\bar{\Omega}/k_t)^{1/2} + k_f m] + \frac{\theta}{2} k_{tc} \left(\int_{i=1}^{j-1} r_i r_{j-i} di + r_1 r_{j-1} \right) \quad (15a)$$

The weight fraction and number and weight average chain lengths are defined as

$$w = \frac{ip_i}{\Sigma ip_i} \quad (16)$$

$$\bar{X}_n = \frac{\Sigma ip_i}{\Sigma p_i} \quad (17)$$

$$\bar{X}_w = \frac{\Sigma i^2 p_i}{\Sigma ip_i} \quad (18)$$

where Σp_i , Σip_i , and $\Sigma i^2 p_i$ are, respectively, the zero-th, first, and second moments of the dead polymer size distribution in the outlet stream. From Equations (5), (6), (7), (8), and (9) it may be shown that the first three moments are

$$\Sigma p_i = \theta(k_{td} + \frac{1}{2} k_{tc})(\bar{\Sigma} r_i)^2 + \theta k_f m \bar{\Sigma} r_i \quad (19)$$

$$\Sigma ip_i = \theta(k_{td} + k_{tc}) \bar{\Sigma} r_i \bar{\Sigma} i r_i + \theta k_f m \bar{\Sigma} i r_i \quad (20)$$

$$\Sigma i^2 p_i = \theta(k_{td} + k_{tc}) \bar{\Sigma} r_i \bar{\Sigma} i^2 r_i + \theta k_{tc} (\bar{\Sigma} i r_i)^2 + \theta k_f m \bar{\Sigma} i^2 r_i \quad (21)$$

where

$$\Sigma r_i = \left[\frac{\bar{\Omega}}{k_t} \right]^{1/2} \quad (22)$$

$$\Sigma i r_i = \frac{\bar{\Omega} + (k_p + k_f)m \Sigma r_i}{k_t \Sigma r_i + k_f m} \quad (23)$$

$$\Sigma i^2 r_i = \frac{\bar{\Omega} + k_p m (\Sigma r_i + 2 \Sigma i r_i) + k_f m \Sigma r_i}{k_t \Sigma r_i + k_f m} \quad (24)$$

Equations (20) and (21) are obtained with the aid of the summation identities

$$\sum_{j=1}^{\infty} j \sum_{i=1}^{j-1} r_i r_{j-i} = 2 \left(\sum_{j=1}^{\infty} r_j \right) \left(\sum_{j=1}^{\infty} j r_j \right)$$

$$\sum_{j=1}^{\infty} j^2 \sum_{i=1}^{j-1} r_i r_{j-i} = 2 \left(\sum_{i=1}^{\infty} r_i \right) \left(\sum_{i=1}^{\infty} i^2 r_i \right) + 2 \left(\sum_{i=1}^{\infty} i r_i \right)^2$$

The above equations were derived for the case of sensitized initiation. It may be shown that they are valid also for the other initiation modes provided the sensitizer concentration is set equal to zero and

$$\Omega(z) = \phi_m I_a(z) \quad \text{for direct photoinitiation}$$

and

$$\Omega(z) = G_R I_a(z) \quad \text{for ionizing radiation initiation.}$$

No Mixing (NM)

For sensitized initiation, material balances for R_1 and R_j in a differential element of reactor volume in the absence of mixing are

$$r_1(z) = \frac{\Omega(z) + k_f m [\Omega(z)/k_t]^{1/2}}{m(k_p + k_f) + [k_t \Omega(z)]^{1/2}} \quad (25)$$

$$r_j(z) = \left[\frac{k_p m}{m(k_p + k_f) + [k_t \Omega(z)]^{1/2}} \right]^{j-1} r_1(z) \quad (26)$$

The sensitizer and monomer are assumed to be perfectly mixed. Thus the concentrations of the sensitizer and the monomer are uniform throughout the reactor and are equal to the outlet concentrations. The material balances for s and m are

$$q s_0 - q s + V \Phi_m = 0 \quad (27)$$

$$q m_0 - q m + V \Phi_m = 0 \quad (28)$$

where Φ_m represents the volume-averaged rate of disappearance of monomer by chemical reaction.

$$\Phi_m = \frac{-2m(k_p + k_f)\theta}{k_t^{1/2}(z_2^2 - z_1^2)} \int_{z_1}^{z_2} z \Omega^{1/2}(z) dz \quad (29)$$

By substituting Equation (29) into (28) and solving for m , we obtain

$$m = \frac{m_0}{1 + \frac{2(k_p + k_f)\theta}{k_t^{1/2}(z_2^2 - z_1^2)} \int_{z_1}^{z_2} z \Omega^{1/2}(z) dz} \quad (30)$$

The material balance for the mixed average concentration of p_j in the reactor effluent is

$$-q p_j + V \Phi_{p_j} = 0 \quad (31)$$

where Φ_{p_j} is the volume-averaged rate of formation of p_j

$$\Phi_{p_j} = \frac{2}{(z_2^2 - z_1^2)} \int_{z_1}^{z_2} \left[k_t d k_t^{-1/2} r_j(z) \Omega^{1/2}(z) + k_f m r_j(z) + \frac{1}{2} k_{tc} \left(\int_{i=1}^{j-1} r_i(z) r_{j-i}(z) di + r_1(z) r_{j-1}(z) \right) \right] z dz \quad (32)$$

Thus

$$p_j = \frac{2\theta}{(z_2^2 - z_1^2)} \int_{z_1}^{z_2} \left[k_t d k_t^{-1/2} r_j(z) \Omega^{1/2}(z) + k_f m r_j(z) + \frac{1}{2} k_{tc} \left(\int_{i=1}^{j-1} r_i(z) r_{j-i}(z) di + r_1(z) r_{j-1}(z) \right) \right] z dz \quad (33)$$

The first three moments of the dead polymer size distribution in the outlet stream are

$$\Sigma p_i = \theta(k_{td} + \frac{1}{2} k_{tc}) [\overline{\Sigma r_i(z)}]^2 + \theta k_f m \overline{\Sigma r_i(z)} \quad (34)$$

$$\Sigma i p_i = \theta(k_{td} + k_{tc}) \overline{\Sigma r_i(z) \Sigma i r_i(z)} + \theta k_f m \overline{\Sigma i r_i(z)} \quad (35)$$

$$\Sigma i^2 p_i = \theta(k_{td} + k_{tc}) \overline{\Sigma r_i(z) \Sigma i^2 r_i(z)} + \theta k_{tc} \overline{[\Sigma i r_i(z)]^2} + \theta k_f m \overline{\Sigma i^2 r_i(z)} \quad (36)$$

where an overlined quantity is the area-averaged value of the quantity over the reactor cross section, and

$$\Sigma r_i(z) = \left[\frac{\Omega(z)}{k_t} \right]^{1/2} \quad (37)$$

$$\Sigma i r_i(z) = \frac{\Omega(z) + (k_p + k_f)m \Sigma r_i(z)}{k_t \Sigma r_i(z) + k_f m} \quad (38)$$

$$\Sigma i^2 r_i(z) = \frac{\Omega(z) + k_p m [\Sigma r_i(z) + 2 \Sigma i r_i(z)] + k_f m \Sigma r_i(z)}{k_t \Sigma r_i(z) + k_f m} \quad (39)$$

The NM equations derived for the case of sensitized initiation again apply in the cases of the two other initiation modes if $s = 0$ and the appropriate definitions of $\Omega(z)$ are used.

In the formulation given above, the chain length j is a discrete variable assuming integer values only. In another approach it may be regarded as a continuous variable*(9). This second approach was also used in the present work for both the PM and NM cases. The resulting equations, which are not shown here, were used in the illustrative calculations that follow. Virtually identical results were obtained with both formulations.

ILLUSTRATIVE CALCULATIONS

The equations derived were used to calculate conversions and molecular weight distributions and averages associated with the polymerization of methyl methacrylate via the three initiation modes. Chemical rate constants used in the calculations are given in Table 1. Since the source

TABLE 1. KINETIC RATE CONSTANTS IN THE POLYMERIZATION OF METHYL METHACRYLATE AT 30°C. (10)

$k_p = 2.86 \times 10^5$ cc./ (g.-mole)(sec.)
$k_f = 0.074$
$k_{tc} = 0.46 \times 10^{10}$
$k_{td} = 1.22 \times 10^{10}$

*By the continuous variable method

$$r_j = r_1 \exp [-(k_t \Sigma r_i + k_f m)(j-1)/(k_p m)]$$

was regarded as infinite in length, reactor height did not enter into the calculations and is not specified. Source well diameter was 3.25 in. ($z_1 = 1.625$ in.). Source well diameter was held constant while source intensity, reactor diameter, flow rate, and state of mixing of chain centers were varied.

Direct Photoinitiation

It was assumed that the effective wavelength range of the ultraviolet light was 300 to 313 $m\mu$, for which Medvedev (11) given in Table 2 and Figures 2 and 3. The examples in the table and figures were constructed for incident intensities of 1×10^{-8} and 1×10^{-6} einstein/(sq. cm.)(sec.). Two reactor diameters, 1 ft. and 4 ft., and two flow rates, corresponding to values of 0.1 and 1 for the ratio of mean residence time to monomer lifetime, were used.

The monomer lifetime is defined in Table 2. It is very long, indicating a very slow reaction and very low flow rates. The radial lifetime is also long, indicating that the perfect mixing state with respect to chain centers may be the significant state. Thus radial mixing times in a 1-ft. or 4-ft. diameter reactor may be short compared with these radical lifetimes.

It may be seen in Table 2 and Figures 2 and 3 that as-

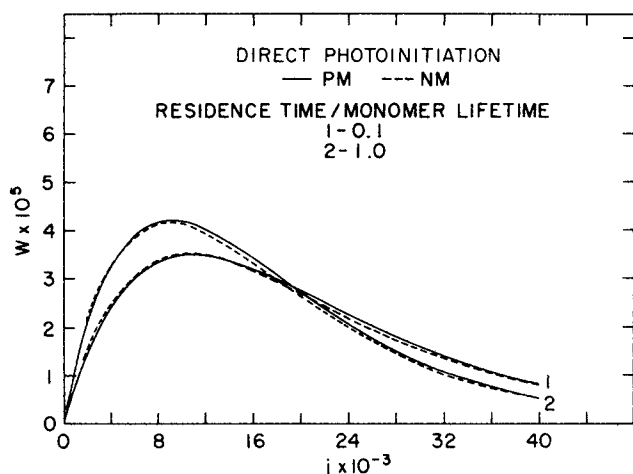


Fig. 2. Molecular weight distributions for direct photoinitiation. $I_0 = 1 \times 10^{-6}$ einstein/(sq. cm.)(sec.). $z_2 = 0.5$ ft.

signment of significance to one or the other mixing state is relatively unimportant since the effect of mixing on all quantities is small. This is because the optical thickness τ for each of the examples is very small, of the order of 10^{-3} . τ is a measure of attenuation by absorption and hence of the nonuniformities in the initiation rate distribution. It is defined in terms of monomer concentration within the reactor. Therefore since conversion is sensitive to mixing state, τ is also.

Fraction conversion increases with mixing as expected (1, 7). The number average chain length \bar{X}_n increases and the weight average \bar{X}_w decreases with mixing, leading to a decrease in polydispersity \bar{X}_w/\bar{X}_n . Exposure, effectively, to a range of intensities in the NM case leads to a broader dispersion than in the PM case, where all elements within the reactor are effectively exposed to a single intensity, namely, the average intensity.

The decrease in average chain length with increased residence time results from increased monomer consumption.

Sensitized Photoinitiation

Depending upon the choice of initiator, its absorption spectrum and its concentration, and on the spectral distribution of the lamp used, one may obtain a very large or very small reactor optical thickness. In the examples given in Table 3 and Figures 4 and 5, conditions were chosen to produce moderately large optical thicknesses. We assumed $\phi_s = 0.6$ mole/einstein, $\alpha_s = 4.3 \times 10^3$, and $s_0 = 9.31 \times 10^{-5}$ mole/cc. The resulting optical thicknesses are 4.45 in the 1-ft. diameter reactor and 22.7 in the 4-ft. diameter reactor. The initiation rate, based on initiator feed concentration and incident intensity, is now relatively high, leading to relatively short monomer and radical lifetimes. The monomer lifetimes are still long compared to any reasonable estimates of mixing times so that the assumption of uniform concentration of monomer throughout each reactor is realistic. The shortness of the radical lifetimes indicates that the significant mixing state for this species will be the NM state.

It is now important to say which mixing state is significant since the effect of mixing on all quantities—fraction conversion, chain length averages, and distributions—is now large. Polydispersities of about 40 are found in the NM state in the large reactors at the high intensities.

The high initiations rates also lead to shorter chain lengths than in the case of direct photoinitiation.

TABLE 2. DIRECT PHOTINITIATION
[$m_0 = 9.31$ mole/liter, $\alpha_m = 0.01$ sq. cm./mole,
 $\phi_m = 0.12$ mole/einstein (11), $z_1 = 1.625$ in.,
 $I_0 = 1 \times 10^{-8}$ einstein/(sq. cm.)(sec.)]

Example		1	2	3	4
z_2 , ft.		0.5	0.5	2	2
θ/θ_m		0.1	1	0.1	1
θ_m , sec.*		1.4×10^6	1.4×10^6	1.4×10^6	1.4×10^6
θ_r , sec.†		23	23	23	23
τ ‡	PM	9.72×10^{-4}	6.80×10^{-4}	5.10×10^{-3}	3.78×10^{-3}
	NM	9.75×10^{-4}	6.82×10^{-4}	5.11×10^{-3}	3.79×10^{-3}
f	PM	0.061	0.345	0.034	0.232
	NM	0.058	0.341	0.032	0.229
\bar{X}_n	PM	103,800	87,000	189,100	169,400
	NM	102,400	86,100	182,200	163,400
\bar{X}_w	PM	203,900	170,900	371,700	332,800
	NM	207,000	173,900	385,000	345,600
\bar{X}_w/\bar{X}_n	PM	1.96	1.96	1.97	1.97
	NM	2.02	2.02	2.12	2.12

$$*\theta_m = 1/[k_p(\phi_m\alpha_m m_0 I_0/k_t)^{1/2}]$$

$$†\theta_r = 1/(k_t\phi_m\alpha_m m_0 I_0)^{1/2}$$

$$‡\tau = \alpha_m m(z_2 - z_1)$$

TABLE 3. SENSITIZED PHOTOINITIATION

$[m_0 = 9.31 \text{ mole/liter}, s_0 = 9.31 \times 10^{-2} \text{ moles/liter}, \alpha_s = 4.3 \times 10^3 \text{ sq.cm./mole}, \phi_s = 0.6 \text{ mole/einstein}, z_1 = 1.625 \text{ in.}, I_0 = 1 \times 10^{-6} \text{ einstein/(sq.cm.) (sec.)}]$

Example	1	2	3	4
z_2 , ft.	0.5	0.5	2	2
θ/θ_m	0.1	1	0.1	1
θ_m , sec.*	9.25×10^2	9.25×10^2	9.25×10^2	9.25×10^2
θ_r , sec.†	0.016	0.016	0.016	0.016
τ ‡	4.45	4.45	22.7	22.7
f_s	1.45×10^{-2}	1.44×10^{-1}	8.5×10^{-4}	8.5×10^{-3}
f				
PM	0.0242	0.1983	0.0059	0.0563
NM	0.0168	0.1526	0.0011	0.0114
\bar{X}_n				
PM	194	160	811	770
NM	134	123	143	142
\bar{X}_w				
PM	379	312	1,590	1,510
NM	552	452	5,670	5,650
\bar{X}_w/\bar{X}_n				
PM	1.96	1.96	1.96	1.96
NM	4.10	3.68	39.7	39.7

$$*\theta_m = 1/[k_p(\phi_s \alpha_s s_0 I_0/k_t)^{1/2}]$$

$$†\theta_r = 1/(k_t \phi_s \alpha_s s_0 I_0)^{1/2}$$

$$‡\tau = \alpha_s s(z_2 - z_1)$$

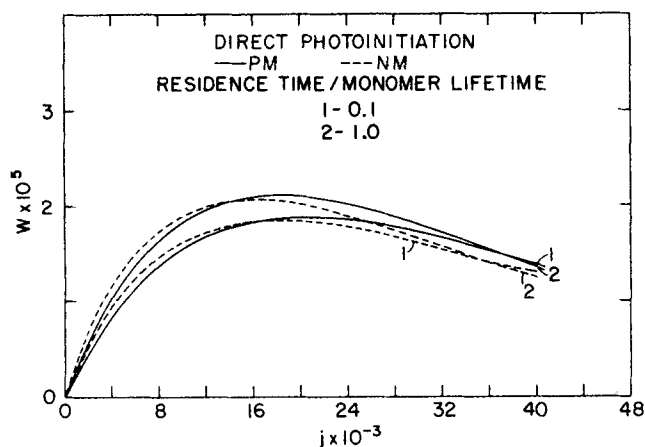


Fig. 3. Molecular weight distributions for direct photoinitiation. $I_0 = 1 \times 10^{-6} \text{ einstein/(sq. cm.) (sec.)}$. $z_2 = 2 \text{ ft.}$

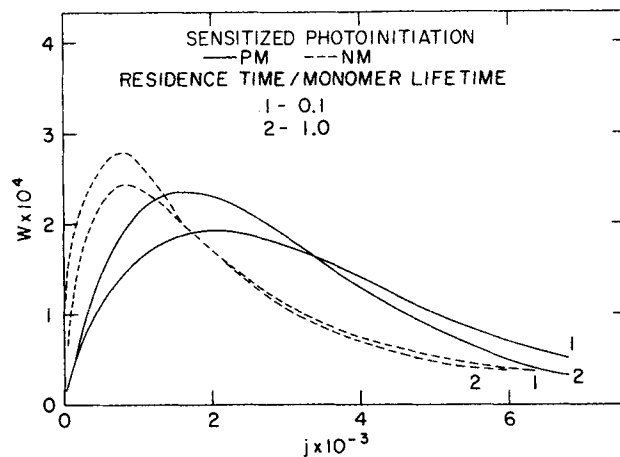


Fig. 4. Molecular weight distributions for sensitized photoinitiation. $I_0 = 1 \times 10^{-8} \text{ einstein/(sq. cm.) (sec.)}$. $z_2 = 0.5 \text{ ft.}$

TABLE 4. IONIZING RADIATION INITIATION

$(m_0 = 9.31 \text{ mole/liter}, \mu = 0.0598 \text{ cm.}^{-1}, G_R \text{ taken from Figure V.10 of ref. 12, } z_1 = 1.625 \text{ in., source strength} = 10 \text{ Ci/cm.)}$

Example	1	2	3	4
z_2 , ft.	0.5	0.5	2	2
θ/θ_m	0.1	1	0.1	1
θ_m , sec.*	4.28×10^4	4.28×10^4	4.28×10^4	4.28×10^4
θ_r , sec.†	0.73	0.73	0.73	0.73
τ ‡	0.665	0.665	3.40	3.40
f				
PM	0.0900	0.4974	0.0364	0.274
NM	0.0882	0.4917	0.0292	0.231
\bar{X}_n				
PM	2,070	1,140	5,720	4,310
NM	2,020	1,130	4,590	3,640
\bar{X}_w				
PM	4,060	2,240	11,200	8,460
NM	4,160	2,320	14,200	11,200
\bar{X}_w/\bar{X}_n				
PM	1.96	1.96	1.96	1.96
NM	2.05	2.05	3.09	3.09

$$*\theta_m = 1/[k_p[(G_R \mu I_0/6.023) \times 10^{-25} k_t]^{1/2}]$$

$$†\theta_r = 1/[k_t(G_R \mu I_0/6.023) \times 10^{-25}]^{1/2}$$

$$‡\tau = \mu(z_2 - z_1)$$

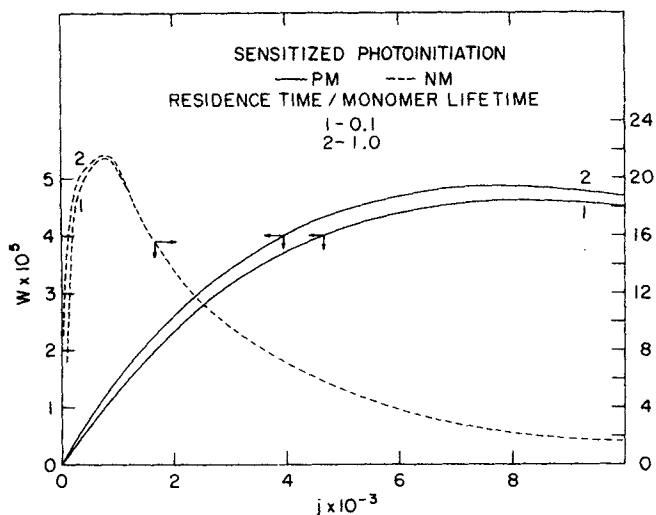


Fig. 5. Molecular weight distributions for sensitized photoinitiation. $I_0 = 1 \times 10^{-8}$ einstein/(sq. cm.)(sec.). $z_2 = 2$ ft.

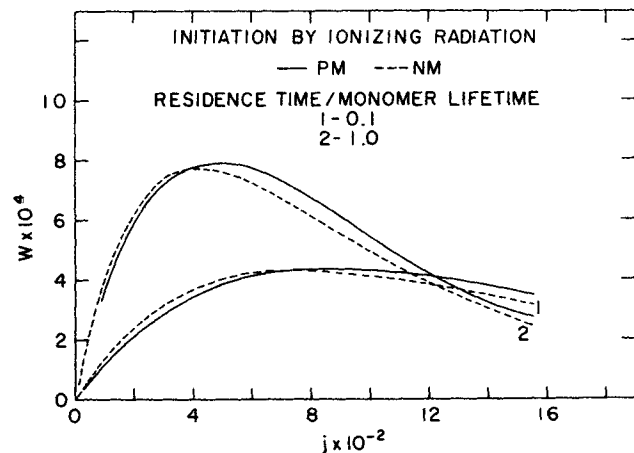


Fig. 6. Molecular weight distributions for ionizing radiation initiation. $S_L = 100$ Ci/cm. $z_2 = 0.5$ ft.

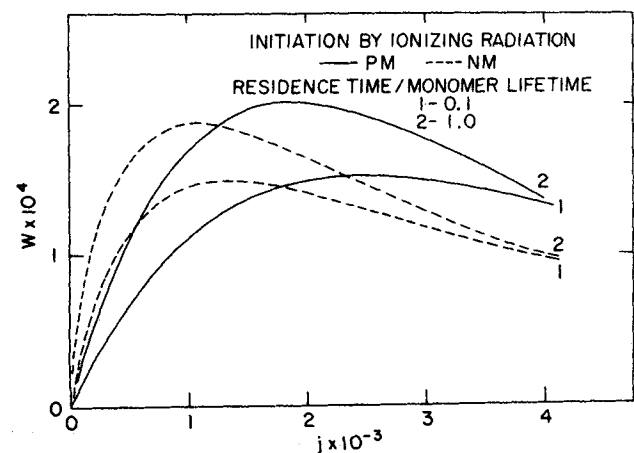


Fig. 7. Molecular weight distributions for ionizing radiation initiation. $S_L = 100$ Ci/cm. $z_2 = 2$ ft.

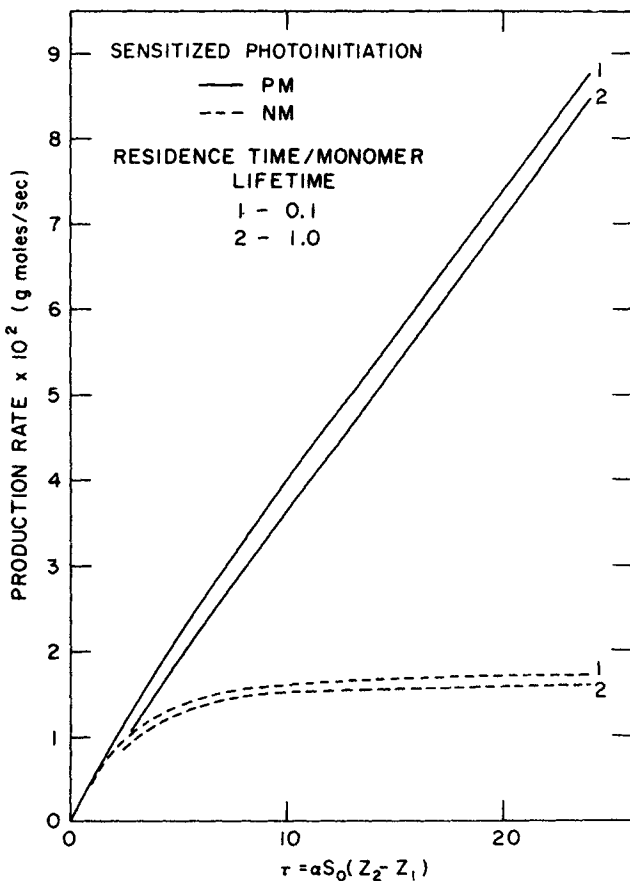


Fig. 8. Production rate for sensitized photoinitiation. $I_0 = 1 \times 10^{-8}$ einstein/(sq. cm.)(sec.).

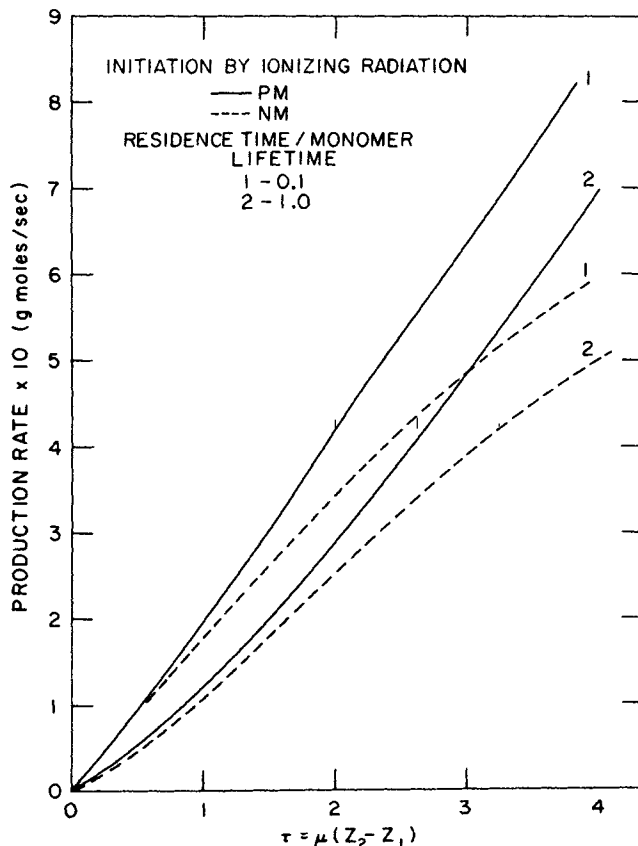


Fig. 9. Production rate for ionizing radiation initiation. $S_L = 100$ Ci/cm.

Ionizing Radiation Initiation

G_R values were taken from Chapiro (12). At low dose rates, a limiting value of 11.5 radicals/100 eV. absorbed exists. Above 1 rad/sec., G_R decreases falling to about 2.3 radicals/100 eV. absorbed at 100 rad/sec. Account was taken of this variation in the calculations. The linear absorption coefficient for Co^{60} gamma rays was taken from Rockwell (6). Source strengths of 10 and 100 Ci/cm were used. The results are given in Table 4 and Figures 6 and 7. In these examples, τ is 0.7 and 3.4. Moderate effects of mixing are seen on all quantities. The NM state is the significant one in view of the short radical lifetimes.

Figures 8 and 9 show the dependence of the rate of production on reactor thickness. The curves for the NM state approach limits as the thickness increases, whereas the perfect mixing curves increase without limit. In the absence of mixing the radicals are confined to the location at which they were produced. Therefore increase in reactor thickness does not affect the concentration profile or rates of production at smaller thicknesses. At sufficiently large thicknesses a negligibly small amount of additional production results from additional increases in thickness and the rate of production approaches a limiting value (1).

CONCLUSION

In each initiation mode it is seen that the transition from the NM to the PM state results in increased fraction conversion, increased \bar{X}_n , decreased \bar{X}_w , and decreased polydispersity. The magnitude of the optical thickness τ determines the relative effect of mixing state. Large values of τ correspond to a large mixing effect and vice versa.

The radical lifetime relative to the mixing time determines which mixing state is significant in practice. A high intensity source yields a short radical lifetime corresponding to significance to the NM state. The opposite result would follow for a low intensity source.

Polymerization reactor performance may thus vary considerably with optical thickness and radical lifetime which are characteristics in part of the initiation mode used.

From a design viewpoint it is important to estimate reactor performance using the NM equations when the radical lifetime is short and the optical thickness is large. When τ is small the PM equations would probably be used regardless of the magnitude of the radical lifetime since there is little effect of mixing state and the PM calculation is simpler to carry out. It is also important to realize that at high optical thicknesses and short radical lifetimes a limiting production rate will be encountered as the reactor is made larger. This limiting rate can only be overcome by increasing the source intensity.

ACKNOWLEDGMENT

This work was supported by the U. S. Atomic Energy Commission and by the Foundation for the Advancement of Graduate Study in Engineering, Newark College of Engineering.

NOTATION

f = fraction conversion of monomer, dimensionless
 f_s = fraction conversion of sensitizer, dimensionless
 G_R = radical yield, radicals/100 eV. absorbed
 h = reactor height, cm.
 I = radiation intensity, einstein/(sq. cm.)(sec.)
 I_0 = incident intensity, einstein/(sq. cm.)(sec.)
 I_a = absorbed intensity, einstein/(cc.)(sec.) or eV./(cc.)(sec.)
 i, j = chain length, dimensionless
 k_f = rate constant for chain transfer to monomer, cc./(g.-mole)(sec.)

k_i = rate constant for reaction of sensitizer radicals with monomer, cc./(g.-mole)(sec.)

k_p = propagation rate constant, cc./(g.-mole)(sec.)

$k_t = k_{tc} + k_{td}$, cc./(g.-mole)(sec.)

k_{tc} = rate constant for termination by combination, cc./(g.-mole)(sec.)

k_{td} = rate constant for termination by disproportionation, cc./(g.-mole)(sec.)

l = distance coordinate along source, as shown in Figure 1

m = monomer concentration in reactor, g.-mole/cc.

m_0 = monomer concentration in feed, g.-mole/cc.

p_j = concentration of dead polymer of chain length j monomer units, g.-mole/cc.

q = volumetric flow rate, cc./sec.

r_j = concentration of active polymer of chain length j monomer units, g.-mole/cc.

s = concentration of sensitizer in reactor, g.-mole/cc.

s_0 = concentration of sensitizer in feed, g.-mole/cc.

S_L = source strength/unit length, Ci/cm.

V = reactor volume, cc.

w = molecular weight distribution function, dimensionless

\bar{X}_n = number average chain length, dimensionless

\bar{X}_w = weight average chain length, dimensionless

z = radial distance, cm.

z_1, z_2 = inner and outer reactor radii, respectively, cm.

Greek Letters

α_m, α_s = molar absorptivities of monomer and sensitizer, respectively, sq.cm./g.-mole

$\theta = V/q$, sec.

θ_m, θ_r = mean lifetime of monomer and radicals, respectively, as defined in Tables 3, 4, and 5, sec.

μ = linear absorption coefficient, cm.⁻¹

τ = reactor optical thickness as defined in Tables 3, 4, and 5, dimensionless

ϕ_m, ϕ_s = primary quantum yield from monomer and sensitizer, respectively, g.-mole/einstein absorbed

Φ_m, Φ_{p_j} = volume averaged rate of disappearance of monomer or of appearance of dead polymer of length j monomer units, respectively, as defined in Equations (29) and (32)

Ω = initiation rate; $\phi_m I_a$ for direct photoinitiation, $\phi_s I_a$ for sensitized initiation, and $(G_R I_a / 6.023) \times 10^{-25}$ for ionizing radiation initiation, g.-mole/(cc.)(sec.)

LITERATURE CITED

- Hill, F. B., and R. M. Felder, *AIChE J.*, **11**, 873 (1965).
- Hill, F. B., and N. Reiss, *Can. J. Chem. Eng.*, **46**, 124 (1968).
- _____, and L. H. Shendalman, *AIChE J.*, **14**, 798 (1968).
- Felder, R. M., and F. B. Hill, *Chem. Eng. Sci.*, **24**, 385 (1969).
- _____, *Ind. Eng. Chem. Fundamentals* **9**, 360 (1970).
- Rockwell, T., ed., "Reactor Shielding Design Manual," p. 342, Van Nostrand, Princeton, N.J. (1956).
- Jacob, S. M., and J. S. Dranoff, paper presented at AIChE Meeting, New York (Dec. 1967).
- Scarborough, J. B., "Numerical Mathematical Analysis," p. 164, Johns Hopkins Press, Baltimore, Md. (1962).
- Zeman, R. J., and N. R. Amundson, *Chem. Eng. Sci.*, **20**, 331, 637 (1965).
- Matheson, M. S., E. B. Bevilacqua, E. E. Auer, and E. J. Hart, *J. Am. Chem. Soc.*, **71**, 497 (1949).
- Medvedev, S. S., *J. Chim. Phys.*, **52**, 677 (1955).
- Chapiro, A., "Radiation Chemistry of Polymeric Systems," p. 184, Interscience, New York (1962).

Manuscript received March 3, 1969; revision received August 22, 1969; paper accepted August 28, 1969. Paper presented at AIChE Cleveland meeting.